16TH EUROPEAN CONFERENCE ON
EARTHQUAKE ENGINEERING THESSALONIKI
18 - 21 JUNE 2018

A MULTI-SCALE METHODOLOGY TO COMPARE SEISMIC HAZARD RESULTS WITH HISTORICAL MACROSEISMIC OBSERVATIONS

Maria ROTA[1], Annalisa ROSTI[2], Andrea PENNA[3], Emilia FIORINI[4], Guido MAGENES[5]

ABSTRACT

This paper presents a multi-scale methodology, developed within the framework of the SIGMA project, to compare probabilistic seismic hazard results with historical macroseismic observations. The comparison is carried out in terms of average annually expected damage (i.e. mean damage). Macroseismic intensities, characterizing the seismic history of a given site, are first converted into an equivalent mean damage catalogue, by implementing a logic tree approach, which allows to handle different sources of uncertainty. On the other side, fragility curves, representative of the seismic vulnerability of the built environment at the time of the historical observations, are employed to generate mean damage values starting from ground motion thresholds, for which PSH estimates are available. PSH outcomes and observations are then compared at different scales, ranging from the site up to regional level. Sampling in space allows to compensate for the lack of macroseismic observations of engineering interest and for the potentially short observation period at individual sites. In this context, two different procedures, differing in the assumption on sites' independence, are outlined. The benefit of aggregating the information available at single sites becomes even more significant when the scale of the comparison is extended to the regional level. The feasibility of the proposed approaches is demonstrated by applications to the South-East quadrant of France.

Keywords: Macroseismic observations; Probabilistic seismic hazard; Macroseismic method, Fragility curves, Sisfrance database

1. INTRODUCTION

Testing probabilistic seismic hazard (PSH) outcomes has become of concern, given the several models and assumptions on which PSH commonly relies on. The adequacy of PSH results can be assessed by employing observations of different type. A natural choice could be the use of accelerometric data (e.g. Ordaz and Reyes 1999; Albarello and D'Amico 2008; Stirling and Gerstenberger 2010; Tasan et al 2014), which are generally affected by small uncertainty. This option could be however of scarce utility, due to the limited lifetime of the recording stations. The observation period could be hence enlarged by using synthetic accelerometric data, which can be generated by coupling earthquake catalogues and ground motion prediction equations (GMPEs) (e.g. Tasan et al. 2014). In this case, the results of the comparison heavily depend on the reliability of the data employed to produce synthetic observations. In countries with long civilization history, an alternative can be represented by macroseismic intensities (e.g. Stirling and Petersen 2006; Labbé 2010). Indeed, although bearing some subjectivity and uncertainty, they can be available for a long time window. Observations of fragile geological structures, such as precarious rocks, may also help to evaluate the accuracy of seismic hazard estimates (e.g. Purvance et al. 2008; Baker et al. 2013).

[1]Researcher, EUCENTRE Foundation, Pavia, Italy, maria.rota@eucentre.it
[2]Post-Doctoral Researcher, University of Pavia, Pavia, Italy, annalisa.rosti@unipv.it
[3]Associate Professor, University of Pavia and EUCENTRE Foundation, Pavia, Italy, andrea.penna@unipv.it
[4]Researcher, EUCENTRE Foundation, Pavia, Italy, emilia.fiorini@eucentre.it
[5]Full Professor, University of Pavia and EUCENTRE Foundation, Pavia, Italy, guido.magenes@unipv.it

Predictions and observations can be easily compared at single sites. However, given the scarcity of the available observations and the short lifetime of recording accelerometric stations, past studies assembled several sites (e.g. Albarello and D'Amico 2008; Stirling and Gerstenberger 2010; Tasan et al. 2014), extending the scale of the comparison up to the regional level (e.g. Labbé 2010).
This paper proposes an innovative multi-scale methodology to compare PSH results with historical macroseismic observations. Comparisons are intended to be performed in terms of the mean damage, μ_D, annually expected in the building stock, at the time of the historical observations. This requires both macroseismic intensities and ground motion intensity thresholds, for which PSH estimates are provided, to be converted into values of mean damage. Predictions and observations are then compared at different scale levels, i.e. at single sites, by aggregating different sites and at the regional scale level. In the latter case, however, the comparison is carried out in terms of PGA. The feasibility of the proposed approaches is demonstrated by an application to the South-East quadrant of France.

2. PROPOSED METHODOLOGY

2.1 Conversion of macroseismic intensities into mean damage values

As sketched in Figure 1, the implementation of the proposed methodology first requires the collection of the seismic events, which stroke the site under investigation, together with the associated macroseismic observations. Furthermore, information on the building stock subdivision into structural typologies is essential for both converting macroseismic intensities into mean damage values and selecting appropriate fragility curves, as described in Section 2.2.
Macroseismic intensities are converted into mean damage values by means of the closed-form analytical formula proposed by Lagomarsino and Giovinazzi (2006) to allow the implementation of the macroseismic method, correlating the expected mean damage, μ_D, and the macroseismic intensity, I:

$$\mu_D = 2.5\left[1 + \tanh\frac{(I+6.25V_i-13.1)}{2.3}\right] \quad (1)$$

where V_i is the vulnerability index.
The equation allows to account for the uncertainty in the attribution of a building typology to the EMS-98 (Grünthal 1998) vulnerability classes. Starting from the corresponding membership function, the macroseismic method defines five vulnerability index values, to account for the probable or less probable behavior of a given typology. The variability of the buildings' characteristics within the same typology could be also taken into account by applying suitable behavior modifiers to the typological vulnerability index.
The outlined methodology permits to account for the uncertainty on the macroseismic intensity values, which may be indicated by some databases of macroseismic observations. This is for instance the case of the Sisfrance database (available at www.sisfrance.net), assigning each observation a different code (i.e. *A*, *B*, *C*), based on the quality of the associated information. To this aim, intensity values are converted into weighted discrete distributions, whose intensity values are identified by normal distributions centered on the intensity level reported in the catalogue. The value of the standard deviation of the normal distribution increases with the uncertainty on the reported intensity value. Each discrete intensity value is then assigned a weight, given by the area bounded by the normal distribution and significant percentiles. For details the reader is addressed to Rosti and Rota (2017).
The conversion of macroseismic intensities into mean damage values is managed by a logic tree approach, allowing to handle different sources of uncertainty involved, such as the possible uncertainty on the reported macroseismic intensity values, the subdivision of the built environment into building typologies and their attribution to the EMS-98 vulnerability classes. For each observed macroseismic intensity, a weighted discrete μ_D distribution is obtained, from which single mean damage values are sampled through a Monte Carlo approach. At each run, the observation period, the best estimate of the empirically-derived annual rates of exceedance (i.e. number of exceedances over the observation period) and its 90% confidence limits are computed for preselected μ_D thresholds. To account for the variability in the different Monte Carlo runs, statistics of the best estimate of the

empirically-derived annual rates of exceedance and of the corresponding confidence bounds are also derived.
The key steps of the proposed methodology to convert the seismic history of a given site into an equivalent mean damage catalogue are illustrated in Figure 1.

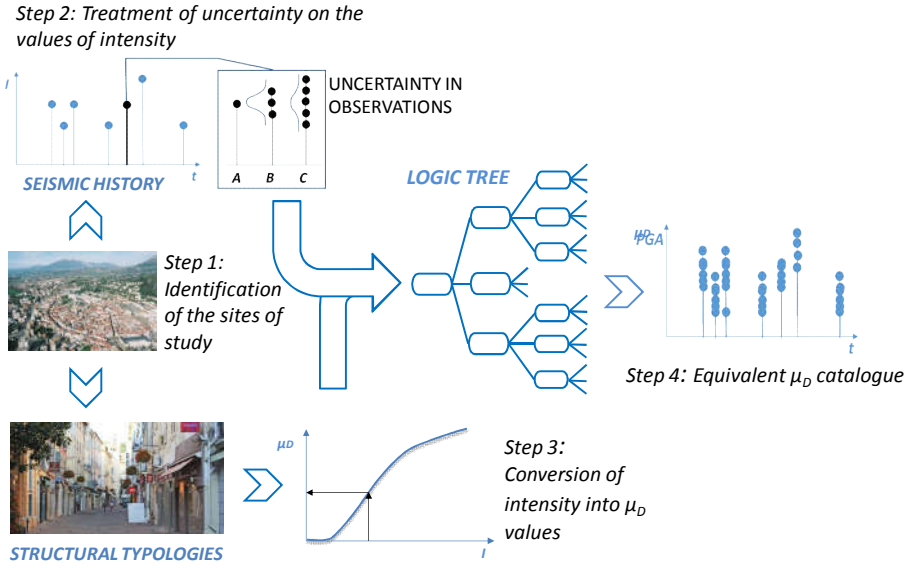

Figure 1. Sketch of the proposed methodology to convert macroseismic intensities into mean damage values (adapted from Rota and Rosti 2017).

2.2 Derivation of mean damage values generated by different PGA thresholds

PSH outcomes generally provide annual rates of exceedance for thresholds of different ground motion intensity measures (*IM*). Therefore, to allow the comparison with historical observations, rates of exceedance need to be associated with μ_D values. As sketched in Figure 2, this is carried out though fragility curves, representative of the seismic vulnerability of the exposed building stock and developed for the same *IM* for which predictions are available. Although the proposed methodology could be easily generalized for any ground motion *IM*, this study refers to PGA, which is often addressed by seismic hazard and vulnerability studies.
A mean damage curve can be computed as a function of the selected *IM* as:

$$\mu_D = \sum_{k=0}^{n} p_k k \qquad (2)$$

where p_k is the probability of occurrence of damage state DS_k ($k = 0 \div n$).
This relation stems from the generally accepted assumption that damage is binomially distributed in n damage levels (e.g. Braga et al. 1982; Lagomarsino and Giovinazzi 2006).
If the building stock in the study area is split into different building typologies, a μ_D-PGA curve has to be generated for each typology. The average of the different μ_D-PGA curves, weighted on the frequency of diffusion of each structural typology, leads to a single μ_D-PGA curve, representative of the whole area. Once mean damage values are linked to PGA thresholds, the association of μ_D values with PSH rates of exceedance is straightforward.

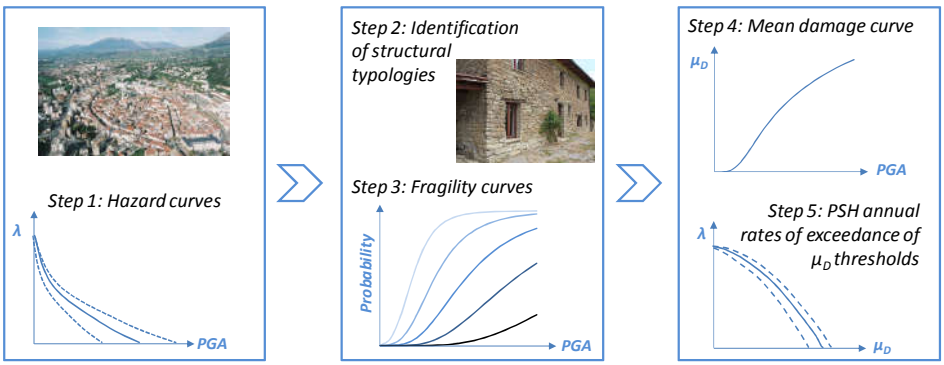

Figure 2. Sketch of the proposed methodology to obtained annual rates of exceedance of mean damage values.

3. MULTI-SCALE COMPARISONS

3.1 Site-specific comparison

PSH outcomes and observations can be immediately compared at the site level, which represents the smallest considered scale. Site-specific comparisons are performed in terms of annual rates of exceedance of preselected μ_D thresholds, by plotting the best estimate of the empirically-derived annual rates and the associated confidence bounds against PSH estimates. Predictions agree with observations if the best estimate of the empirically-derived annual rates of exceedance fall within selected percentiles of PSH results.

3.2 Comparison on aggregated sites

Site-specific comparisons are affected by the seismic history of the selected site. Sparse and/or low entity macroseismic observations, together with a potentially short time window, may indeed impede pertinent comparisons. These issues and limitations could be tackled by sampling in space. In other words, time and space are swapped, under the commonly accepted assumption of the ergodicity of the process of earthquakes' occurrence. Several sites are hence aggregated and treated as a single one, allowing to make up for the scarcity of observations at a given location. In this context, a possible issue could be represented by the stochastic dependency of observations, generated by the same earthquake at different sites (Iervolino and Giorgio 2015). Based on these considerations, two procedures, differing in the assumption on sites' independence, are proposed in the following.

3.2.1 Sites' aggregation assuming sites' independence

The proposed approach compares the observed and predicted number of sites with exceedance of preselected μ_D thresholds, under the assumption of sites' independence, i.e. stochastic independence of the observations generated at different sites by the same seismic event. Sites to be aggregated are selected to be sufficiently far from each other, so that exceedances at different sites can be considered stochastically independent.
For each site, a μ_D catalogue is generated starting from its seismic history, in accordance with Section 2.1, and mean damage values are then sampled from each equivalent μ_D seismic history. Potential dependent observations are checked at each Monte Carlo run and possibly removed, by discarding the lowest μ_D value produced by the earthquake at different locations. The distribution of the observed number of sites with exceedance is then derived for each preselected mean damage threshold.
On the other side of the comparison, the expected mean number of exceedances, N_{mean}, is computed for each selected site as:

$$N_{mean} = T_{obs} \cdot \lambda \tag{3}$$

In the formula, T_{obs} is the observation period, calculated when sampling mean damage values from the equivalent catalogue, whereas λ denotes the PSH-derived rate of exceedance.
The epistemic uncertainty in the hazard can be taken into account by sampling rates of exceedance from a lognormal distribution approximating the different percentiles of the PSH estimates, for a given μ_D threshold. Additional details are reported in Rota and Rosti (2017).
Similarly to Tasan et al. (2014), the probability of observing n mean damage values above the selected threshold is computed, assuming that the process of occurrence of earthquakes can be described as a Poisson process:

$$P(n) = \frac{(N_{mean})^n \cdot e^{-N_{mean}}}{n!} \quad (4)$$

For each site, numbers of exceedances compatible with the PSH model are generated by sampling from the associated Poisson distribution (Figure 3). At each run, the expected number of sites with exceedance is calculated by summing the sites with at least one exceedance. A distribution of the expected number of sites exceeding the preselected mean damage threshold is derived, together with relevant statistics. Predictions meet observations if the latter fall within the percentiles of the expected distribution.

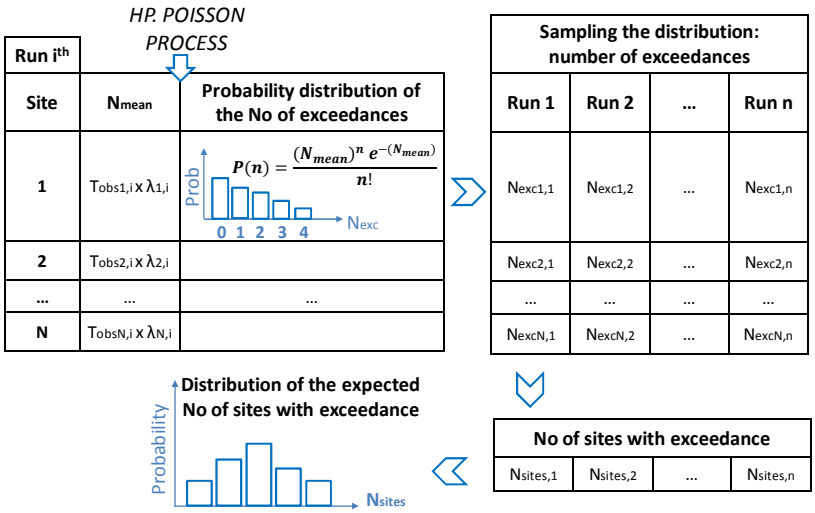

Figure 3. Sketch of the procedure to generate number of exceedances compatible with the PSH model. Calculation of the number of sites with exceedance and of its distribution for a given mean damage threshold (adapted from Rota and Rosti 2017).

3.2.2 Sites' aggregation avoiding the assumption on sites' independence

Since neglecting the stochastic dependency does not impact the mean but only the variance of a distribution of results (Iervolino and Giorgio 2015), the comparison can be performed on a set of sites in terms of mean annual rates of exceedance in at least one site, with the advantage of avoiding any assumption on the stochastic independency. The implementation of this alternative procedure requires the following steps:

1. Generation of the equivalent μ_D catalogue and sampling of mean damage values from the corresponding distribution, in accordance with Section 2.1. This step needs to be applied to all the selected sites.
2. Calculation of empirically-derived mean annual rates of exceedance of all sites for preselected μ_D thresholds. For a given μ_D level, the mean annual rate of exceedance in at least one site is then given by the sum of the empirically-derived mean annual rate of exceedance of each site, divided by the total number of sites to be aggregated.
3. Sampling of annual rates of exceedance from the lognormal distribution fitting the different PSH percentiles at preselected μ_D levels and calculation of the expected mean annual rate of exceedance

in at least one site, similarly to step 2.
4. Comparison of empirically- and PSH-derived mean annual rates of exceedance in at least one of the sites.

3.3 Comparison at the regional scale

Previous comparisons demonstrated that the size of the usable observational dataset can be considerably enlarged by collecting and assembling the information available at single sites. The scale of the comparison is thus extended to study region, to make up for issues related with the lack of macroseismic observations. With respect to the previous approaches, a further improvement consists in generating spatially correlated ground motion random fields, constrained on the available macroseismic observations, with the advantage of integrating the seismic histories and possibly solving some completeness issues (e.g. missing or uncertain observations). The reader is addressed to Park et al. (2007) for a detailed description of the procedure to derive conditional ground motion random fields. The implementation of the proposed methodology requires the following steps:

1. Identification of the sites to be aggregated.
2. Selection of the seismic events to be considered for the generation of ground motion random fields.
3. Generation of spatially correlated PGA random fields, constrained on the available macroseismic observations. To this aim, a GMPE and a spatial correlation model are necessary.
4. Comparison of empirically- and PSH-derived mean annual rates of exceedance in at least one of the sites, similarly to Section 3.2.2.

4. APPLICATION TO THE SOUTH-EAST QUADRANT OF FRANCE

This Section applies the outlined methodologies to the South-East quadrant of France. Based on the available information on the building stock at the time of the historical observations, four structural typologies were identified, all including undressed stone masonry buildings with flexible horizontal structure, only differing in the number of stories (i.e. 1-2 and >2) and presence of connecting devices (i.e. tie-rods and tie-beams). Each typology was assigned a weight, depending on the environmental context (Figure 4).

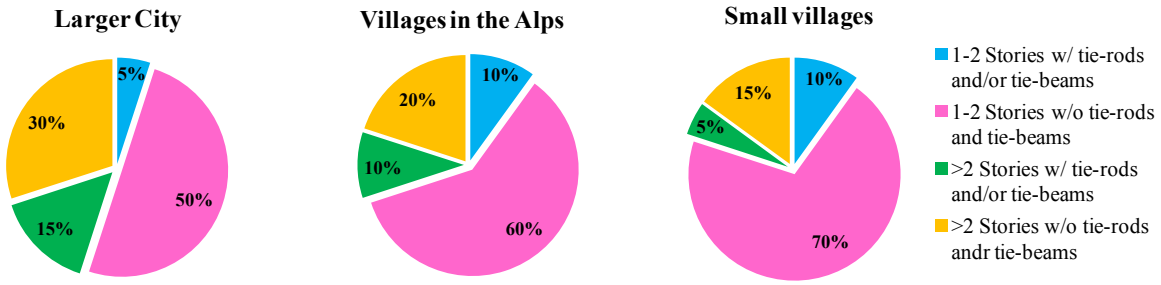

Figure 4. Building stock subdivision into structural typologies, based on the environmental context.

4.1 Application of site-specific comparison

The feasibility of site-specific comparisons is demonstrated with reference to the city of Nice. Figure 5 (left) reports the observed macroseismic intensities, five of which exceed intensity level V (i.e. slight crack in the plasterwork, according to the MSK-64 scale, Medvedev et al. 1964). According to Sisfrance, a macroseismic observation of intensity level VIII was associated to the 1887 Western Liguria event. This intensity value, which is at least two intensity degrees higher than the other observations, is however affected by secondary effects, described as tsunami. Based on the considerations discussed in Rosti et al. (2014), this intensity value was modified to VII, consistently with the MCS intensity degree reported by the parametric catalogue of Italian earthquakes (Rovida et al. 2016). In Figure 5 (centre), each macroseismic observation of Figure 5 (left) is replaced by a

weighted discrete intensity distribution, depending on the reliability of each observation (i.e. *A*: certain observation; *B*: fairly certain and *C*: uncertain). Details on the definition of the normal distributions and of weights assigned to the different intensity levels are reported in Rosti and Rota (2017). Figure 5 (right) shows the equivalent mean damage catalogue resulting from the implementation of the logic tree approach, in accordance with Section 2.1. It can be observed that a weighted discrete μ_D distribution corresponds to each macroseismic observation of Figure 5 (left).

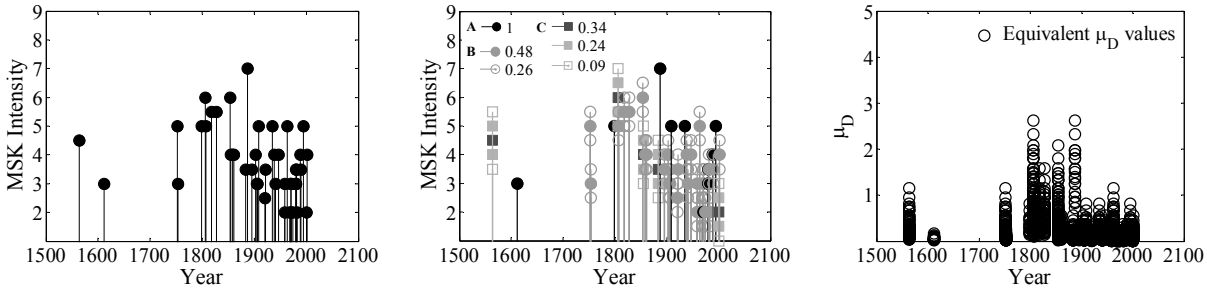

Figure 5. Seismic history (left), modified seismic history (centre) and equivalent μ_D catalogue (right) of Nice.

On the other side of the comparison, μ_D values were generated from PGA thresholds, by using empirical fragility curves, derived from the statistical elaboration of post-earthquake damage data collected after Italian earthquakes (Rosti and Rota 2017). Mean damage thresholds were then associated with the PSH annual rates of exceedance provided by Carbon et al. (2012). Figure 6 compares the best estimate (dark grey) and 90% confidence bounds (black and light grey, respectively) of the empirically-derived annual rates of exceedance of μ_D thresholds with different percentiles of PSH estimates. Markers correspond to the average (diamonds) and median (circles), whereas error bars indicate the variability within the different Monte Carlo runs (i.e. 5th and 95th percentiles). PSH outcomes are in agreement with observations, starting from a μ_D threshold of 1.5, given that the best estimate of the empirically-derived rates of exceedance fall within predictions. At lower μ_D thresholds, predictions overestimate observations. The uncertainty on the best-estimate of the empirically-derived rates of exceedance is smaller at lower μ_D levels, probably due to the considerable number of low mean damage values of the equivalent mean damage catalogue (Figure 5, right). By contrast, at higher μ_D thresholds, the uncertainty on the empirically-derived rates of exceedance appears to be excessively large. The effect of the different sources of uncertainty on the results is deeply investigated in Rosti and Rota (2017), with reference to another case study.

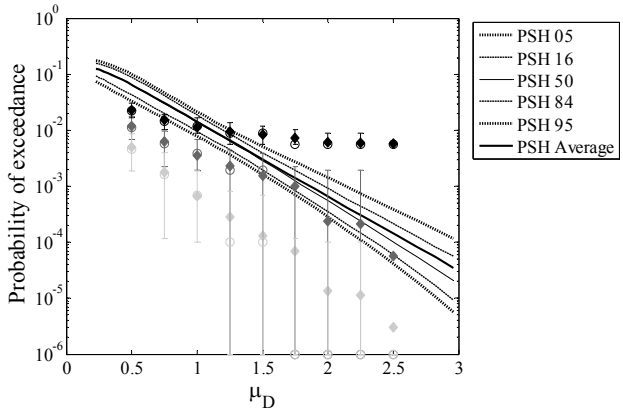

Figure 6. Comparison of different percentiles of PSH estimates with statistics of the best estimate (dark grey) and of the upper (black) and lower (light grey) 90% confidence limits of the empirically-derived annual rates of exceedance. Diamonds: average; circles: median, error bars: 5th and 95th percentiles.

4.2 Application to a set of sites

PSH estimates and observations were compared on a set of seven sites, located in the study area (i.e. Annecy, Albertville, Draguignan, Beaumont de Pertuis, Digne, La Mure and L'Argentières La Bessée). Exceedances at the different sites could be assumed to be produced by independent seismic events, given that sites are sufficiently far from each other (Figure 7). To account for the building stock subdivision into different typologies, Annecy and Draguignan were considered larger cities, Albertville and La Mure villages in the Alps, whereas the remaining sites were assigned to the class of smaller villages (Figure 4).

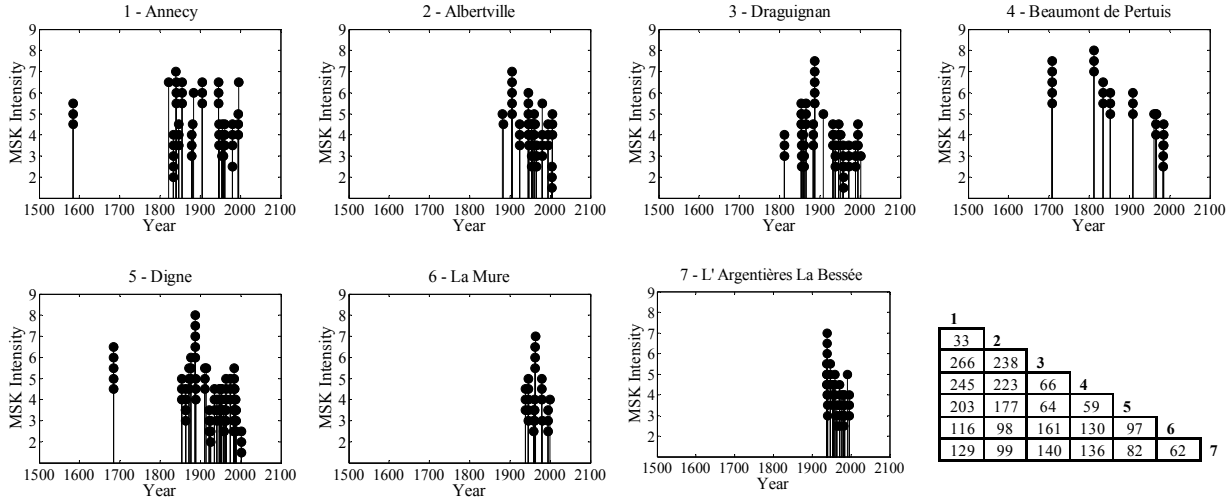

Figure 7. Seismic histories of the selected sites, accounting for the uncertainty on the macroseismic intensities and geodetic inter-site distance in km (Rosti and Rota 2017).

In accordance with Section 2.1, for each site an equivalent mean damage catalogue was generated, from which μ_D values were sampled from the corresponding weighted discrete distribution. The observed number of sites with exceedance was thus derived for mean damage levels from 0.5 to 2.75, with step of 0.25, after checking and removing possible observations generated by the same earthquake at different sites. The expected number of sites with exceedance and meaningful statistics were also derived for each μ_D level, in accordance with Section 3.2.1.

As an example, Figure 8 compares the observed (red bars) and expected (white bars) distribution of the number of sites with exceedance, for μ_D thresholds of 1.5 (left) and 2.5 (right). In these specific cases, PSH are consistent with observations, which fall within the selected percentiles of the expected distribution. Results for all μ_D thresholds are reported in Rosti and Rota (2017). Figure 9 (left) summarizes the results of the comparisons, in terms of statistics of the number of sites with exceedance for the preselected mean damage levels. To provide an order of magnitude of ground motion values associated with the different μ_D levels, the comparison is also shown in terms of PGA (Figure 9, right).

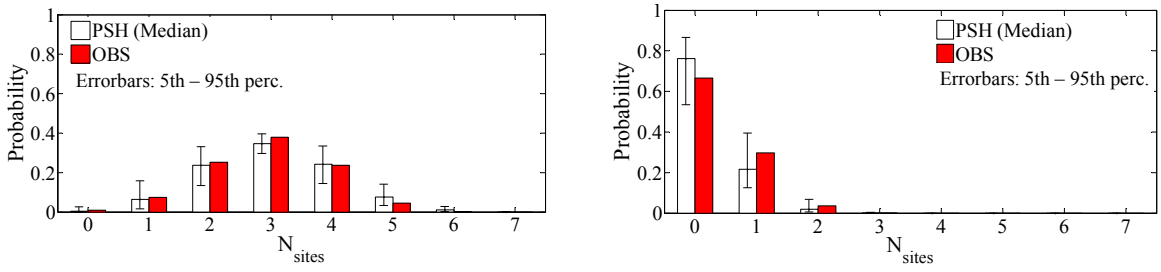

Figure 8. Comparison of the expected (from PSH) and observed distribution of the number of sites with exceedances for mean damage thresholds 1.5 (left) and 2.5 (right).

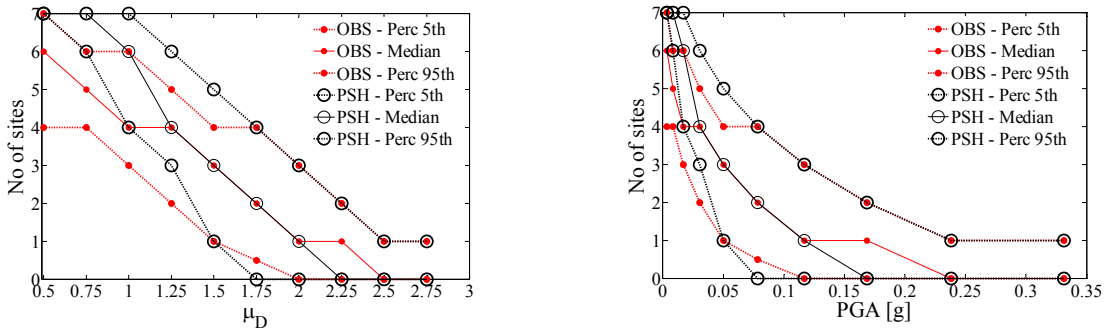

Figure 9. Comparison of the expected and observed number of sites with exceedance for all preselected mean damage thresholds (left) and corresponding PGAs (right). (Adapted from Rosti and Rota 2017).

Sites were also aggregated in accordance with the approach of Section 3.2.2, which does not require any assumption on sites' independency. The results of the comparison in terms of mean annual rates of exceedance in at least one of the site are depicted in Figure 10. PSH estimates are consistent with observations staring from mean damage level of 1.5, whereas they tend to overestimate observations at lower μ_D thresholds. As already pointed out, this outcome may be ascribed to some low entity macroseismic observations missing in the catalogue. The comparison does not however seem to be reasonable for μ_D levels smaller than 1, corresponding to very low PGA values and macroseismic observations of intensity level lower than VI (and therefore less reliable).

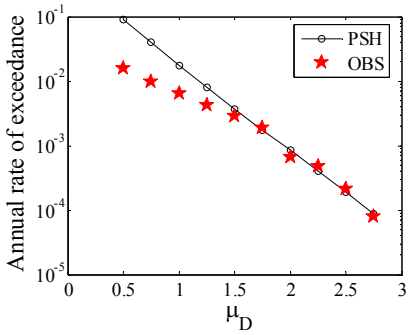

Figure 10. Comparison of the empirically- (red stars) and PSH-derived (black) mean annual rates of exceedance of μ_D thresholds in at least one of the sites (adapted from Rosti and Rota 2017).

4.3 Application of the regional comparison

The scale of the comparison was finally extended to the whole South-East French quadrant, including eleven departments (Figure 11, left). To this aim, 580 grid points, approximately spaced at 10 km within the area study and for which PSH estimates were available (Carbon et al. 2012), were aggregated. PGA random fields were generated on rock, consistently with the hazard study to be tested, by using the Akkar et al. (2014) GMPE and the spatial correlation model by Jayaram and Baker (2009). Site conditions were evaluated based on the USGS $V_{s,30}$ map (Wald and Allen 2007). Synthetic observations were produced at the selected locations for 196 earthquakes, with moment magnitude ranging from 4 to 6.62. The dataset of seismic events included independent shocks, producing macroseismic intensity observations at least equal to IV within the study area and with minimum epicentral intensity of V. For consistency with the selected GMPE, only seismic events with minimum moment magnitude of 4 and within 200 km from the hazard grid were considered. The left part of Figure 11 shows the epicenter location of each selected seismic event, with different colors corresponding to different magnitude ranges (i.e. green: 4≤M<5; yellow: 5≤M<6; red: M≥6). On the right, the epicentral intensity of the selected earthquakes is plotted versus time, using the same colors.

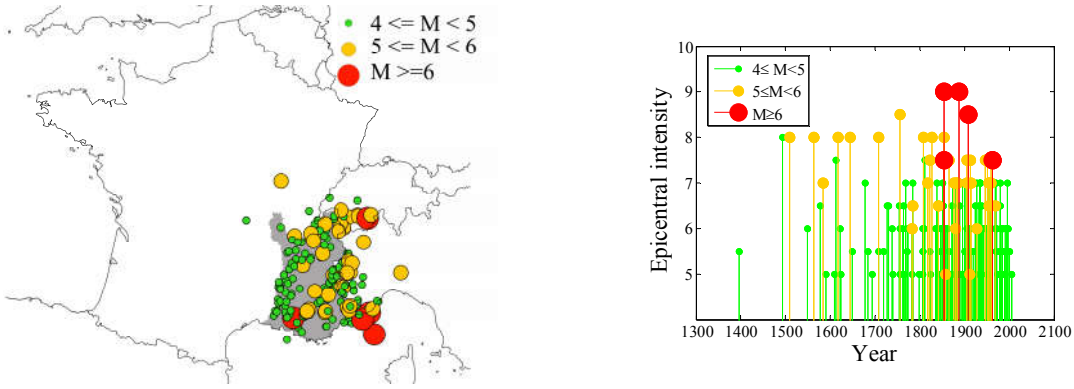

Figure 11. France map with indication of the region of study (grey area) and epicenter location of the selected seismic events, with indication of the magnitude range (left); epicentral intensity versus time of the selected seismic events (right).

For each seismic event, the simulation of ground motion random fields resulted in lognormal PGA distributions at the selected locations, compatible with both earthquake characteristics and the available macroseismic observations. Figure 12 shows the comparison between empirically- and PSH-derived mean annual rates of exceedance in at least one of the sites, up to 0.5g. A good agreement between predictions and observations was observed in the PGA range 0.1-0.5g, whereas, at lower PGAs, PSH outcomes overestimate observations.

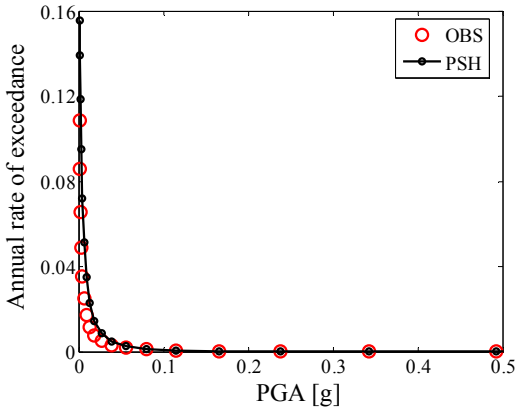

Figure 12. Comparison of the empirically-derived (red stars) and PSH-derived (black) mean annual rates of exceedance of mean damage thresholds in at least one of the sites.

5. CONCLUSIONS

This paper presents a multi-scale methodology to compare PSH outcomes with historical macroseismic observations, with specific application to the South-East quadrant of France. The comparison is performed in terms of the average damage annually expected in the built environment at the time of observations. To this aim, both macroseismic intensities and ground motion intensity thresholds, for which PSH estimates are available, are converted into mean damage values. Predictions and observations are first compared at the site level, in terms of annual rates of exceedance of mean damage thresholds. Although immediate, site-specific comparisons are affected by sparse and/or limited entity observations. To counteract this issue, several sites are aggregated, by applying two procedures, which differ in the assumption on sites' independence. The scale of the comparison is further extended to exploit all the information available within the study region. Differently from the previous approaches, PGA random fields, constrained on the available macroseismic observations, are generated, with the advantage of supplementing the available seismic histories. Although the unquestionable benefit of enlarging the size of the available dataset, the regional comparison can only test the agreement between PSH predictions and observations on average.

6. ACKNOWLEDGMENTS

This work was developed within the framework of the project SIGMA, under the financial support of Areva. The authors acknowledge Mr. J.M. Thiry of Areva, Dr. G. Senfaute of EDF, Dr. Ch. Martin of Geoter and Prof. P. Bazzurro of Institute of Advanced Study (IUSS) Pavia for several discussions on the topic. Very helpful revisions of a previous version of the work were provided by Prof. E. Faccioli, Dr. A. Gurpinar, Dr. G. Woo and Dr. J. Savy. The authors also would like to acknowledge Dr. S. Giovinazzi for her help with the application of the macroseismic method and Prof. I. Iervolino for valuable suggestions on a specific part of this work

7. REFERENCES

Akkar S, Sandikkaya MA, Bommer JJ (2014) Empirical ground-motion models for point- and extended- source crustal earthquake scenarios in Europe and the Middle East. *Bull Earthq Eng*, 12(1): 359-387.

Albarello D, D'Amico V (2008) Testing probabilistic seismic hazard estimates by comparison with observations: an example in Italy. *Geophys J Int*, 175: 1088-1094.

Baker JW, Abrahamson NA, Whitney JW, Board MP, Hanks TC (2013) Use of fragile geologic structures as indicators of unexceeded ground motions and direct constraints on probabilistic seismic hazard analysis. *Bull Seismol Soc Am*, 103(3): 1898-1911.

Braga F, Dolce M, Liberatore D (1982) A statistical study on damaged buildings and an ensuing review of the M.S.K.-76 scale. *Proceedings of the 7th European Conf Earthq Eng*, Athens, Greece.

Carbon D, Drouet S, Gomes C, Leon A, Martin C, Secanell R (2012) Probabilistic analysis for France's southeast ¼ to produce a "classical" hazard map. *Deliverable SIGMA-2012-D4-24, Final Report.*

Grünthal G (ed.), Musson RMW, Schwarz J, Stucchi M (1998). European Macroseismic Scale. Cahiers du Centre Européen de Géodynamique et de Séismologie, Vol. 15, Luxembourg.

Iervolino I, Giorgio M (2015) The effect of dependence of observations on hazard validation studies. *CSNI Workshop on Testing PSHA Results and Benefit of Bayesian Techniques for Seismic Hazard Assessment*, Pavia, Italy.

Jayaram N, Baker JW (2009) Correlation model for spatially distributed ground-motion intensities. *Earthq Eng Struct Dyn*, 38(15): 1687-1708.

Labbé PB (2010) PSHA outputs versus historical seismicity. Example of France. *Proceedings of the 14th European Conf Earthq Eng*, Ohrid, Macedonia.

Lagomarsino S, Giovinazzi S (2006). Macroseismic and mechanical models for the vulnerability and damage assessment of current buildings. *Bull Earthq Eng*, 4: 415-443.

Medvedev S, Sponheuer W, Karnik V (1964) Neue seismische Skala Intensity scale of earthquakes, 7. Tagung der Europäischen Seismologischen Kommission vom 24.9. bis 30.9.1962. In: Jena, Veröff. Institut für Bodendynamik und Erdbebenforschung. Deutsche Akademie der Wissenschaften, 77: 69-76.

Ordaz M, Reyes C (1999) Earthquake hazard in Mexico City: observations versus computations. *Bull Seismol Soc Am*, 89(5): 1379-1383.

Park J, Bazzurro P, Baker JW (2007) Modeling spatial correlation of ground motion intensity measures for regional seismic hazard and portfolio loss estimation. *Proceeding of the 10th International Conf on Application of Statistic and Probability in Civil Engineering*, Tokyo, Japan.

Purvance M.D, Brune JN, Abrahamson NA, Anderson JG (2008) Consistency of precariously balanced rocks with probabilistic seismic hazard estimates in Southern California. *Bull Seismol Soc Am*, 98(6): 2629-2640.

Rosti A, Rota M (2017). Comparison of PSH results with historical macroseismic observations at different scales. Part 2: application to South-East France. *Bull Earthq Eng*, 15(11): 4609-4633.

Rosti A, Rota M, Fiorini E, Penna A, Bazzurro P, Magenes G (2014) Development and implementation of a method to compare PSHA results to historical observations using fragility curves. Revised version of *Deliverable D4-118*.

Rota M, Rosti A (2017). Comparison of PSH results with historical macroseismic observations at different scales. Part 1: methodology. *Bull Earthq Eng*, 15(11): 4585-4607.

Rovida A, Locati M, Camassi R, Lolli B, Gasperini P (eds) (2016) CPTI15, the 2015 version of the Parametric Catalogue of Italian Earthquakes. Istituto Nazionale di Geofisica e Vulcanologia. doi:http://doi.org/10.6092/INGV.IT-CPTI15.

Stirling M, Gerstenberger M (2010) Ground motion-based testing of seismic hazard models in New Zealand. *Bull Seismol Soc Am*, 100(4): 1407-1414.

Stirling M, Petersen M (2006) Comparison of the historical record of earthquake hazard with seismic-hazard models for New Zealand and the Continental United States. *Bull Seismol Soc Am*, 96(6): 1978-1994.

Tasan H, Beauval C, Helmstetter A, Sandikkaya A, Guéguen, P (2014) Testing probabilistic seismic hazard estimates against accelerometric data in two countries: France and Turkey. *Geophys J Int*, 198(3): 1554-1571.

Wald DJ, Allen TI (2007) Topographic slope as a proxy for seismic site conditions and amplification. *Bull Seismol Soc Am*, 97(5): 1379-1395.